Model-free information-theoretic approach to infer leadership in pairs of zebrafish

Sachit Butail, Violet Mwaffo, and Maurizio Porfiri

A model-free information-theoretic approach to infer leadership in pairs of zebrafish

Sachit Butail,[1, *] Violet Mwaffo,[2] and Maurizio Porfiri[2]

[1]*Indraprastha Institute of Information Technology Delhi (IIIT-Delhi), New Delhi, India*
[2]*Department of Mechanical and Aerospace Engineering,*
New York University Tandon School of Engineering, Brooklyn, NY, USA

Collective behavior affords several advantages to fish in avoiding predators, foraging, mating, and swimming. Although fish schools have been traditionally considered egalitarian superorganisms, a number of empirical observations suggest the emergence of leadership in gregarious groups. Detecting and classifying leader-follower relationships is central to elucidate the behavioral and physiological causes of leadership and understand its consequences. Here, we demonstrate a new information-theoretic approach to infer leadership from positional data of fish swimming. In this framework, we measure social interactions between fish pairs through the mathematical construct of transfer entropy, which quantifies the predictive power of a time series to anticipate another, possibly coupled, time series. We focus on the zebrafish model organism, which is rapidly emerging as a species of choice in preclinical research for its genetic similarity with humans and reduced neurobiological complexity with respect to mammals. To overcome experimental confounds and generate test datasets on which we can thoroughly assess our approach, we adapt and calibrate a data-driven stochastic model of zebrafish motion for the simulation of coupled dynamical system of zebrafish pairs. In this synthetic dataset, the extent and direction of the coupling between the fish is systematically varied across a wide parameter range to demonstrate the accuracy and reliability of transfer entropy in inferring leadership. Our approach is expected to aid in the analysis of collective behavior, providing a new, data-driven perspective to understand social interactions.

* sbutail@iiitd.ac.in

I. INTRODUCTION

Fish collective behavior captivates the interest of the general public and scientific community for its beauty, spontaneity, and complexity. Schooling in fish is ubiquitous across a range of species [1] and begets several advantages, such as predator avoidance [2] and energy savings [3]. Although fish schools have traditionally been considered as egalitarian superorganisms [4, 5] in which collective behavior emerges through self-organization, recent studies have proposed differences among individuals to be essential for the group coordination [6, 7]. Beyond behavioral and physiological factors, leadership may emerge due to the possession of knowledge that may benefit the group. This knowledge could be the location of a food source or a predator in the environment [8–10], and could depend on the relative position and nutritional state of an individual [11], possibly linked to strength of social bonds and personality traits [12–14].

To identify leadership in fish shoals, a classical approach is to look for trajectories that are similar within a finite time lag using cross-correlation [11]. Within such an approach, it is expected that leaders will exhibit anticipatory turns [11, 15], not necessarily from the front [11, 12, 16], which are then followed by the rest of the group members with some response latency. Cross-correlation, however, assumes a linear dependence, and is sensitive to noise [17]. Further, the assumption of an underlying model, the inherent stochasticity of the group response, and varying time delays caused by speed changes [18] hamper the possibility of robustly inferring directed leader-follower relationships.

We posit an alternative model-free approach toward inferring leader-follower relationships through the measurement of the amount of information transfer within pairs of individuals. This concept is grounded in information theory, where the notion of information is modeled using a theoretic construct called entropy [19]. Entropy of a random variable quantifies the degree of uncertainty in predicting its value. For example, if the fish orientation is represented as a random variable, a turn, compared to straight swimming, would represent higher uncertainty. In an information theoretic sense, this implies that turns impart more entropy to the fish trajectory.

Once the time evolution of a given system is represented using a stochastic process, the information flow between a pair of such systems can be used to pinpoint leader-follower relationships, in which net information is transferred from one system (leader) to the other (follower). Leaders are thus expected to play a causal role on the followers [20], which would imply that the orientation of a follower fish is driven by the orientation of the leader fish. Model-free measures such as transfer entropy or conditional mutual information are often utilized to quantify information flow and help infer causality between the systems. These and related information theoretic measures have contributed to an improved understanding of the dynamics of complex networks [20–22], neuronal connectivity in brain [23, 24], and causal relationships in weather forecasting [25], stock market analysis [26], social media [27], and animal behavior [28–31].

Toward generating datasets that are free from experimental uncertainties where leadership roles may be inconsistent or time-varying, we adapt a stochastic model of zebrafish (*Danio rerio*) locomotion [32] to include pairwise interactions [33] and calibrate it using empirical data. Zebrafish is an emerging animal model and a species of choice in preclinical research for its genetic similarity with humans and reduced neurobiological complexity with respect to mammals [34–36]. Being a highly social organism, it holds a key similarity to humans in its tendency to interact with conspecifics [34, 37]. Different from larger teleosts, zebrafish swimming is composed of sporadic bursts of the tail that are followed by coasting phases, during which zebrafish swim forward without beating their tail [38–40]. This burst-and-coast swimming style results in a complex time evolution for their body orientation, in which large spikes in the turn rate (sudden changes of the orientation) are superimposed to small fluctuations [32, 41, 42]. Social behavior in zebrafish is measured in the form of preference [37], cohesion [43], and coordination [39, 44] among individuals, and is often associated with efficient foraging and anti-predator advantages.

We test the hypothesis that information transfer, measured through the notion of transfer entropy, can be used to identify leader-follower relationships in zebrafish. The extent and direction of the leader-follower coupling between the fish is systematically varied across a wide parameter range to demonstrate the accuracy and reliability of transfer entropy in inferring leadership. We compare our information-theoretic model-free approach with classical time lag analysis, based on cross-correlation, and extreme-event synchronization [45].

The outline of the paper is as follows. In Section II, we introduce the notion of transfer entropy and detail its use in quantifying information flow between two dynamical systems. Section III provides a background on the method of extreme-event synchronization. We then describe the zebrafish swimming model in two dimensions (2D) with pairwise interactions in Section IV. In Section V, we classify the relationships between simulated pairs of zebrafish using transfer entropy extreme event synchronization and cross-correlation. In Section VI, we present a further study, where we analyze the effect of variations in the coupling gains on each of the classification measures considered in Section V. We discuss open challenges that should be addressed to extend these results to groups of more than two zebrafish in Section VII, and conclude in Section VIII with a summary of main results and future work.
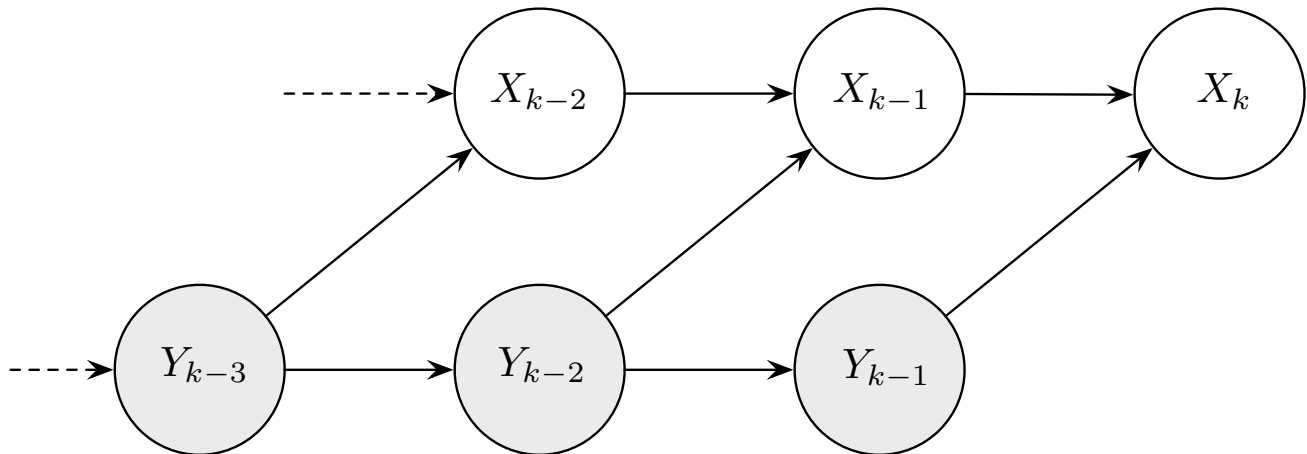
II.   QUANTIFYING INFORMATION TRANSFER

FIG. 1. Transfer entropy quantifies the relationship between two processes X and Y, where knowledge of one process reduces the uncertainty in the other. In the example above, arrows denote direction of information flow, where process Y is said to cause the process X in the sense of Granger [54], where past values of Y helps predict future values of X.

In information theory, the amount of uncertainty contained in a random variable X is quantified using the entropy $H(X)$ defined as [55]

$$H(X) = -\sum_{x \in \mathcal{X}} p(x) \log p(x), \tag{1}$$

where $p(x) = P(X = x)$ is the probability of X taking the value x in the set $\mathcal{X}$ containing all the possible realizations of X. The joint and conditional entropy of two random variables X and Y are similarly defined as [55]

$$H(X, Y) = -\sum_{x \in \mathcal{X}, y \in \mathcal{Y}} p(x, y) \log p(x, y),$$
$$H(X|Y) = -\sum_{x \in \mathcal{X}, y \in \mathcal{Y}} p(x, y) \log p(x|y). \tag{2}$$

Information in this sense can be interpreted as "a measure of how much choice is involved in the selection of the event or of how uncertain we are of the outcome" [19], and high uncertainty implies more information. Two random variables that are not independent are expected to share common information. This quantity is called the mutual information

$$I(X; Y) = H(X) + H(Y) - H(X, Y). \tag{3}$$

Mutual information is symmetric, that is, $I(X; Y) = I(Y; X)$. Conditional mutual information, which quantifies the shared information between X and Y, given another variable Z is computed as [56]

$$I(X; Y|Z) = H(X|Z) + H(Y|Z) - H(X, Y|Z). \tag{4}$$

We employ transfer entropy to measure information transfer between pairs of simulated and experimental fish. Using X, and Y to denote different time series, modeled as stochastic processes $\{X_k\}_{k \in \mathbb{N}}$, and $\{Y_k\}_{k \in \mathbb{N}}$, transfer entropy $\mathrm{TE}_{Y \to X}$ is an asymmetric quantity that measures the reduction in uncertainty of predicting X_k given Y_k. Transfer entropy represents the mutual information between Y_k and X_k conditioned on a previous instance of X_k

assuming the processes are Markov chain of order one [56, 57]. Specifically [55]

$$
\begin{aligned}
\mathrm{TE}_{Y \to X} =& \sum_{\substack{x_k \in \mathcal{X}_k, \\ x_{k-1} \in \mathcal{X}_{k-1}, \\ y_{k-1} \in \mathcal{Y}_{k-1}}} p(x_k, x_{k-1}, y_{k-1}) \log \frac{p(x_k | x_{k-1}, y_{k-1})}{p(x_k | x_{k-1})} \\
=& I(Y_{k-1}; X_k | X_{k-1}) \\
=& H(Y_{k-1} | X_{k-1}) + H(X_k | X_{k-1}) \\
& - H(Y_{k-1}, X_k | X_{k-1}) \\
=& H(X_k | X_{k-1}) - H(X_k | X_{k-1}, Y_{k-1}),
\end{aligned}
\tag{5}
$$

where $p(x_k | x_{k-1}, y_{k-1})$ denotes the probability of x_k given x_{k-1} and y_{k-1}. Net transfer entropy is computed as $\mathrm{TE}_{Y \to X} - \mathrm{TE}_{X \to Y}$. This quantity is used in our work to infer causal, leader-follower relationships between the systems, whereby net transfer entropy would be positive if Y is driving X, that is, if Y is a leader and X a follower.

Transfer entropy is measured by estimating the joint probability densities in (5) using binning methods [56] or kernel density estimators [58]. A binning approach is sensitive to bin width, which controls the amount of smoothing, and the start point of the first bin, which affects the shape of the histogram [59]. To guarantee robustness of results over varying bin-widths, we computed transfer entropy over a range of bin widths varying between 0.03–0.40.

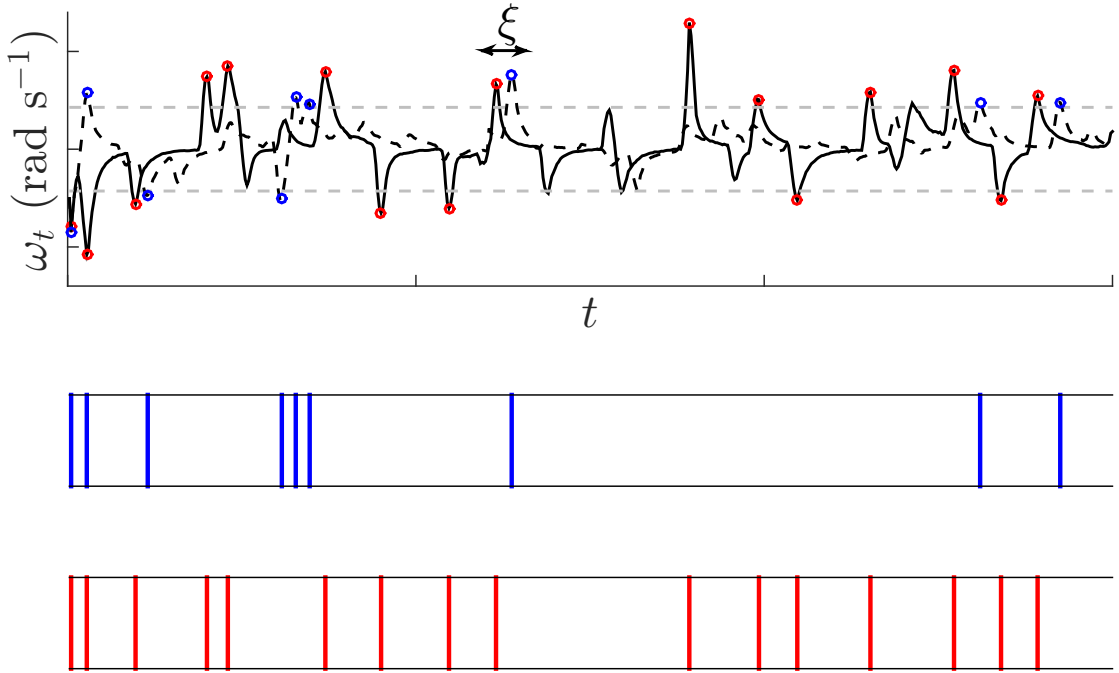## III.   QUANTIFYING SYNCHRONICITY AND EVENT DELAY BETWEEN EXTREME EVENTS

FIG. 2. Extreme-event synchronization quantifies the synchronicity between extreme events in two processes with varying delays. Two extreme events within ξ time of each other are considered synchronous.

Extreme-event synchronization is used to measure the synchronicity between extreme events and is robust to varying delays [45, 60]. For a pair of time series, X, and Y, a second set of time series denoting extreme events only, may be constructed by setting a threshold. Specifically, we assemble a new pair of series t_i^x and t_j^y, $i = 1, \ldots, m_x$ and $j = 1, \ldots, m_y$, where t_i^x denotes the i-th instance where the value of X crossed the set threshold. Given a time lag ξ

that is permitted between two synchronous extreme events, the quantity [45]

$$c^\xi(X|Y) = \sum_{i=1}^{m_x}\sum_{j=1}^{m_y} J_{ij}^\xi, \tag{6}$$

where

$$J_{ij}^\xi = \begin{cases} 1 & \text{if } 0 < t_i^x - t_j^y \le \xi \\ 1/2 & \text{if } t_i^x = t_j^y \\ 0 & \text{otherwise,} \end{cases}$$

counts the number of extreme events in Y that occur immediately prior to an extreme event in X. Similarly, $c^\xi(Y|X)$ counts the number of times an extreme event appears in X shortly before in Y. The symmetric and asymmetric quantities [45]

$$Q_\xi = \frac{c^\xi(Y|X) + c^\xi(X|Y)}{\sqrt{m_x m_y}}; \ q_\xi = \frac{c^\xi(Y|X) - c^\xi(X|Y)}{\sqrt{m_x m_y}} \tag{7}$$

capture the event synchronicity and event delay between the extreme events in the pair of time series. In particular, $0 \le Q_\xi \le 1$, where $Q_\xi = 1$ implies that the events are completely synchronous, and $-1 \le q_\xi \le 1$, where $q_\xi = 1$ implies that extreme events in X always occur prior to those in Y.

IV. MODELING ZEBRAFISH INTERACTIONS

Following [32, 41, 46], we model each zebrafish as a jump persistent turning walker (JPTW). Briefly, zebrafish turn rate is modeled as a stochastic mean-reverting jump diffusion process, where the turn rate tends to revert towards its mean in the long term under the influence of noise [47]. The rate of reversion and the degree of stochasticity are parameterized through a linear time decay and an additive noise, with the latter composed of a jump process superimposed on a Wiener process that model the burst-and-coast swimming style. The JPTW is extended to model fish pairs by incorporating response functions in the diffusion process, so that the mean turn rate of each fish would not decay to zero but to a value that is controlled by the relative location of the other fish [33, 48, 49].

Specifically, denoting the instantaneous 2D position of zebrafish $i = 1, 2$, at time t by $\mathbf{r}_t^{(i)}$, and orientation by $\phi_t^{(i)}$ (rad), for constant speed $v^{(i)}$ $(\mathrm{cm\,s^{-1}})$, the fish motion is described by

$$\dot{\mathbf{r}}_t^{(i)} = v^{(i)} \begin{bmatrix} \cos\phi_t^{(i)} \\ \sin\phi_t^{(i)} \end{bmatrix}; \ \dot{\phi}_t^{(i)} = \omega_t^{(i)}, \tag{8}$$

where a superimposed dot indicates derivative with respect to time. The instantaneous turn rate $\omega_t^{(i)}$ $(\mathrm{rad\,s^{-1}})$ evolves according to a stochastic differential equation [32]

$$d\omega_t^{(i)} = -\eta^{(i)}\left(\omega_t^{(i)} - {}^*\omega_{t-\tau}^{(i)}\right)dt + \sigma^{(i)}dW_t^{(i)} + dJ_t^{(i)}, \tag{9}$$

where $\eta^{(i)}$ $(\mathrm{s^{-1}})$ is the reversion rate; ${}^*\omega_{t-\tau}^{(i)}$ $(\mathrm{rad\,s^{-1}})$ is the response function [33]; $\tau = 10$ ms is the response latency which is related to the time required to complete a turn [50]; $dW_t^{(i)}$ are increments of a standard Wiener process corresponding to zero-mean Gaussian random variables with time-increment dt as variance; $\sigma^{(i)}$ $(\mathrm{rad\,s^{-3/2}})$ scales the noise intensity of the Wiener process[1]; $J_t^{(i)}$ is the jump term modeled as a compounded Poisson process, such that $J_t^{(i)} = \sum_{k=1}^{\nu_t} Z_k^{(i)}$, where $\nu_t - \nu_r$, where $r \le t$, is a Poisson random variable with parameter $\lambda^{(i)}(t - r)$, $\lambda^{(i)}$ $(\mathrm{s^{-1}})$ being the frequency of jumps; and $Z_k^{(i)}$ is a zero-mean Gaussian random variable with variance $\left(\gamma^{(i)}\right)^2$ $(\mathrm{rad^2\,s^{-2}})$.

To compute the response function, we denote the instantaneous distance between the two fish by $d_t = \left\lVert \mathbf{r}_t^{(1)} - \mathbf{r}_t^{(2)} \right\rVert$, the relative orientation of fish j with respect to fish i by $\phi_t^{(i,j)} = \phi_t^{(j)} - \phi_t^{(i)}$, and the angular position of j with respect

---

[1] Note the unfortunate typo in [32, 41, 49, 51], where the units of noise intensity are erroneously written as $\mathrm{rad\,s^{-1}}$.
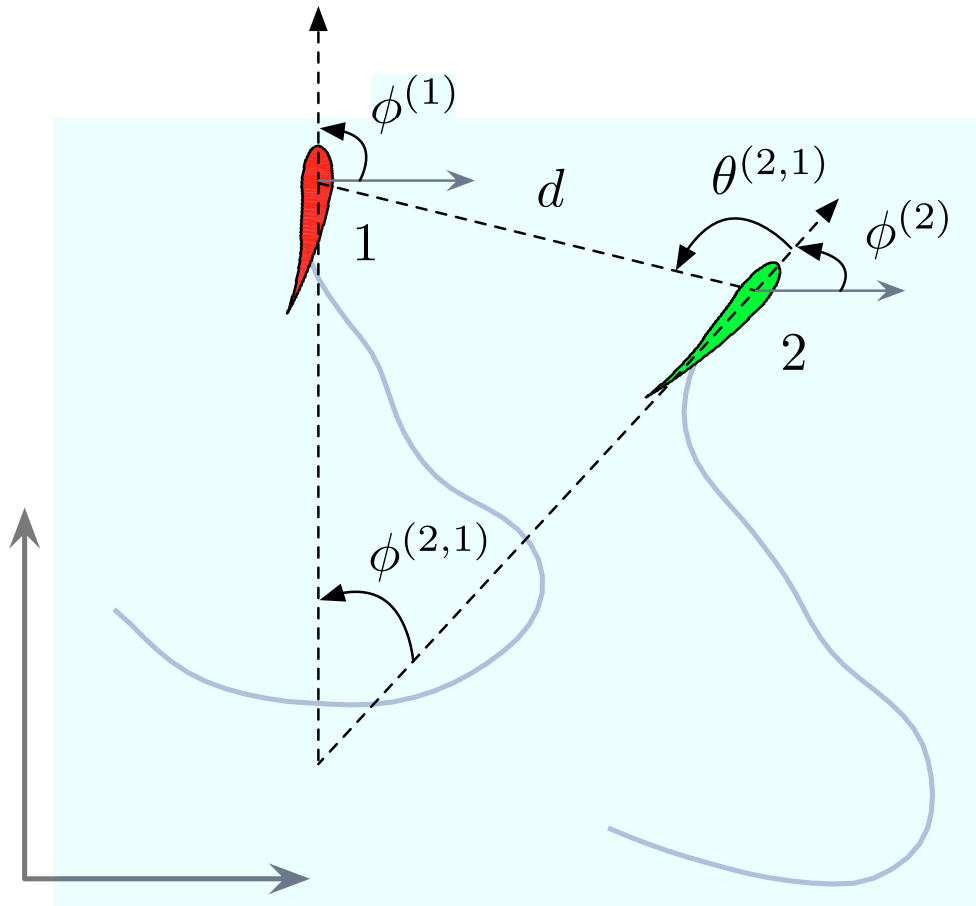
FIG. 3. Schematic of a zebrafish pair with superimposed notation.

to i by $\theta_t^{(i,j)}$ (Fig. 3). The response function is

$$
\begin{aligned}
{}^*\omega_{t-\tau}^{(i)} = \left[1 + \cos\left(\theta_{t-\tau}^{(i,j)}\right)\right] & \left[k_v^{(i)} v^{(i)} \sin\left(\phi_{t-\tau}^{(i,j)}\right) + \right. \\
& \left. k_p^{(i)} d_{t-\tau} \sin\left(\theta_{t-\tau}^{(i,j)}\right)\right],
\end{aligned}
\tag{10}
$$

where $k_p^{(i)}$ $\left(\mathrm{rad\,m^{-1}s^{-1}}\right)$ and $k_v^{(i)}$ $\left(\mathrm{rad\,m^{-1}}\right)$ are the gain parameters for attraction and alignment respectively [33]. Different from [49, 51], the speed is assumed to be constant in time irrespective of the relative position of the fish with respect to each other. To simulate leader-follower pairs, with fish i as the leader, $k_p^{(i)}$ and $k_v^{(i)}$ are set to zero [52]. For leaderless pairs, $k_p^{(1)} = k_p^{(2)}$ and $k_v^{(1)} = k_v^{(2)}$.

V. CLASSIFYING PAIRS OF SIMULATED ZEBRAFISH

In a first simulation study, the gains k_p and k_v are each fixed to contrast fish behavior in the presence and absence of a leader, and thus assess the accuracy of each method to detect leaders in zebrafish pairs. The values $k_p = 5.72\,\mathrm{rad\,m^{-1}s^{-1}}$ and $k_v = 31.9\,\mathrm{rad\,m^{-1}}$ for the follower fish are chosen to exemplify a strong coupling between the fish, whereby these are the largest values we observed in our model calibration (details in Appendix A).

Simulations of zebrafish pairs are run according to equations (8–10), integrated using Euler-Maruyama approximation [53], with a time-step length of 10 ms for 120 seconds each. The role of leader is attributed to a particular fish by setting its coupling strength gains to zero, representing unidirectional interaction (Fig. 4). Since transfer entropy estimation from time-series is sensitive to sampling rate [28, 61], the sensitivity is determined by estimating
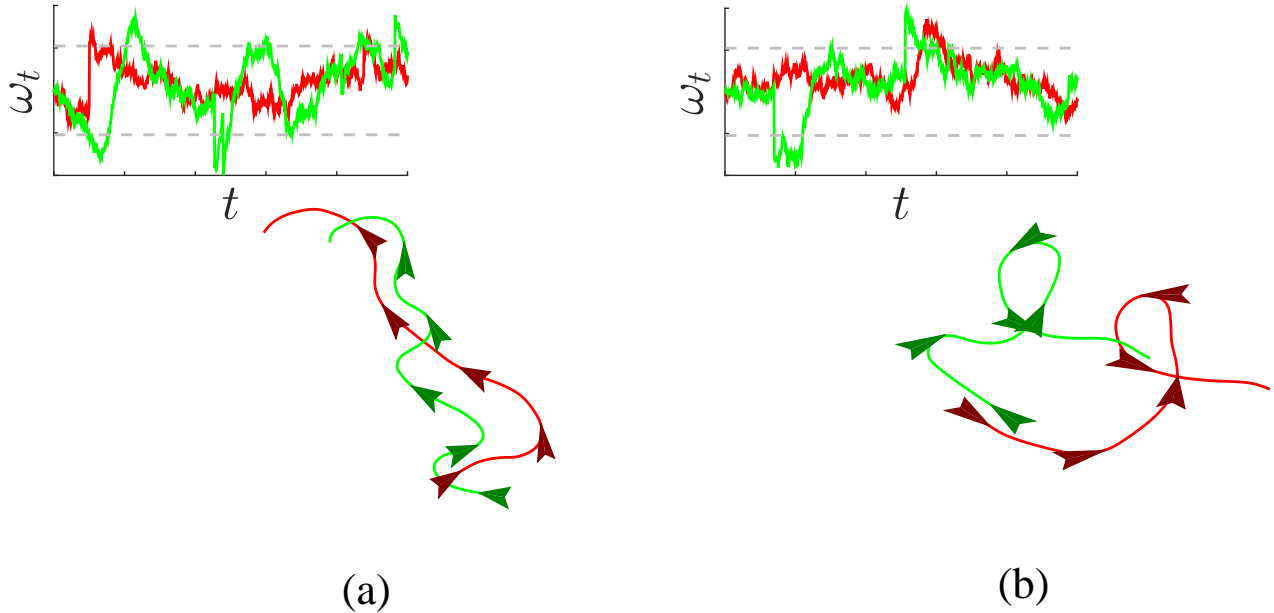
FIG. 4. Sample time trace trajectories of simulated fish, 10 seconds long, for leader-follower (a) and leaderless (b) pairs, with corresponding turn rates in the inset. Arrows are marked at the same instants in time for each fish.

the conditional entropy for different sampling rates. A sampling time (different from the simulation time-step length) of 0.2 seconds is selected, which marks the value beyond which there is no significant increase in conditional entropy (Fig. B1). All model parameters, except the coupling gains for alignment and attraction, are sampled uniformly from a range within one standard deviation of the average values obtained after fitting the model to experimental data (details in Appendix A). For computing transfer entropy, the X and Y processes in (5) are selected as $\sin\left(\phi_t^{(1)}\right)$ and $\sin\left(\phi_t^{(2)}\right)$, where the sine serves to wrap the value of the orientation smoothly within a $[-1, 1]$ range, ensuring that the density functions share the same support [58]. For extreme-event synchronization, fish turn rates are processed to create the time series t_i^x and t_j^y by isolating extreme values for each fish. Specifically, a threshold equal to three times the standard deviation over the average noise intensity is used to index the times when extreme events occurred. These time series are then used to compute event synchronicity Q_ξ and event delay q_ξ as in (7). The value of ξ for which successive peaks in the turn rates of different fish should be considered synchronous is set to 20 ms. This value corresponds to the sum of the response latency and the time required by a fish to attain its maximum angular velocity during a turn [50].

In addition to the methods of transfer entropy and extreme-event synchronization, we also evaluate the datasets with classical time lag analysis using cross-correlation. To compute time lag, fish orientation trajectories are split into two-second segments and cross-correlated to obtain the time lag that maximized the cross-correlation [15]. The average time lag $t_\times$ across segments is used to infer the anticipation of swimming direction by a single fish. A negative value, for example, when fish 1 trajectory is cross-correlated with fish 2, implies that on average fish 1 orientation preceded that of fish 2.

The different methods for inferring leadership—time lag from cross-correlation, event delay from extreme-event synchronization, and net transfer entropy—are compared by using the value from each method as a classifier on 200 datasets, 100 each for leader-follower pairs and leaderless pairs, obtained by setting $k_p = 5.72\,\mathrm{rad\,m^{-1}s^{-1}}$ and $k_v = 31.9\,\mathrm{rad\,m^{-1}}$ for both. For each method, a threshold value of time lag, event delay, and net transfer entropy is selected to assess a pair. Note that a leaderless pair can be classified falsely as leader-follower in either direction; thus the magnitude of the classifier is first used to differentiate leaderless from leader-follower pairs. Specifically, for each of the classifiers, the absolute value of the measure is tested against a selected threshold to identify the existence of a leader-follower pair and then the prediction of which of the fish is a leader, or follower, is compared with the ground truth.

For example, in the case of cross-correlation, a fish pair is classified as leader-follower if the absolute time lag is

more than a given threshold; once established, the sign of the time lag is used to check for a true or false positive. Similarly, in the case of event-synchronization, a threshold on the event delay is utilized to classify leader-follower pairs. Finally, with net transfer entropy as a classifier, first the bin-width that results in maximum difference between leader-follower pair and leaderless pairs over the range of bin-widths is identified, and then a threshold on the value of net transfer entropy for that bin-width is used to identify leader-follower pairs.

To evaluate the dependency of the performance on the threshold value, a range of thresholds values are selected for each classifier based on the extremes beyond which there is no appreciable change in accuracy. The minimum value of threshold is set to 0.01 for all classifiers to be consistent with the simulation time-step length. The accuracy of a classifier at a given threshold is defined as [62]

$$Acc = \frac{\text{true positive + true negative}}{\text{total number of test datasets}}. \tag{11}$$

The accuracy at each threshold is in turn used to create a receiver operating characteristic (ROC) curves of the three classifiers [62]. An ROC curve provides a visual analysis of the accuracy of a classifier by plotting the true positive rate versus false positive rate for a range of thresholds. Points on the diagonal at 45° represent 50% accuracy, implying that the classifier is able to discriminate between true and false positives only half the time. Points away from the diagonal towards upper left corner represent better accuracy.
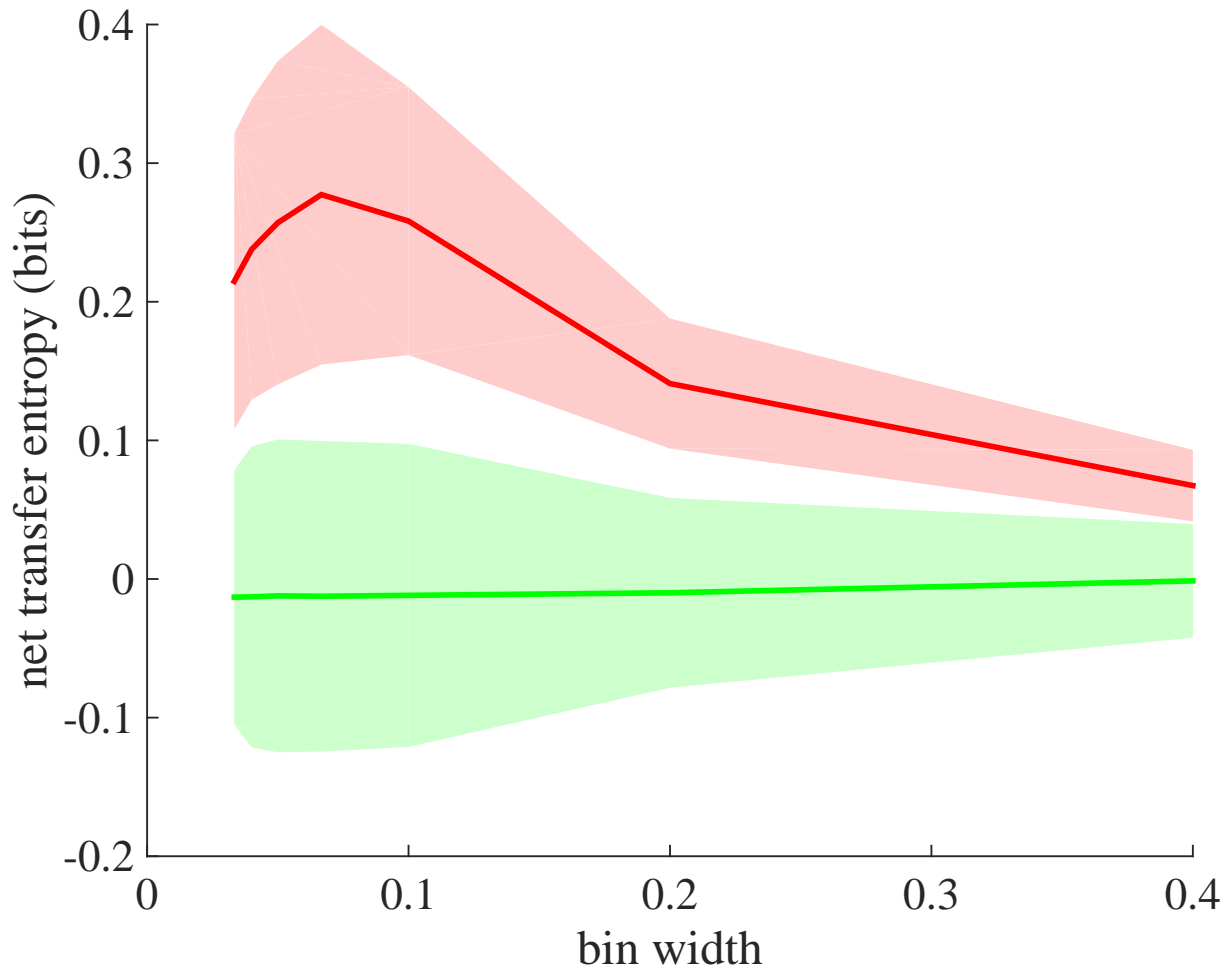

FIG. 5. Net transfer entropy ($\text{TE}_{\text{leader}\rightarrow\text{follower}} - \text{TE}_{\text{follower}\rightarrow\text{leader}}$) at different bin widths for simulations with leader-follower (red) and leaderless (green) pairs. Error envelopes denote standard deviation over 100 simulations each.

The net information transfer as measured by the difference in transfer entropy is more for leader-follower than leaderless pairs (Fig. 5). This result holds across all bin widths, with the maximum difference at bin-width 0.1. Net transfer entropy at this bin width is used to classify leader-follower relationships.
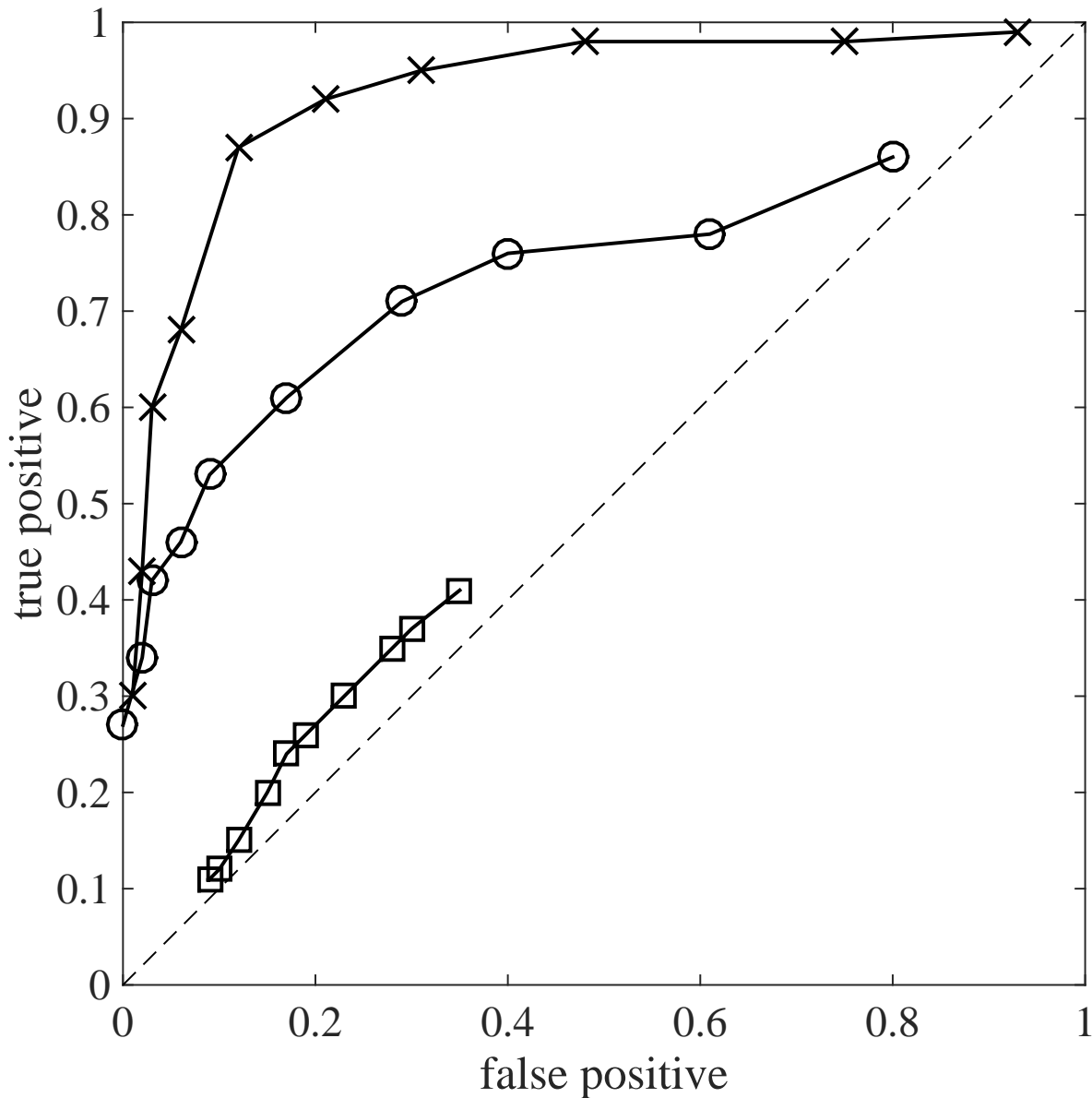
FIG. 6. ROC curves for event delay from extreme-event synchronization (□), time lag from cross-correlation (◦), and net transfer entropy (×). Points closer to the diagonal (dashed) are less accurate than points towards top and left borders. Net transfer entropy is the most accurate at 87.5% for a threshold of 0.17.

Figure 6 compares the three classifiers—time lag, event delay, and net transfer entropy—across different thresholds for inferring the presence of leadership using ROC curves (accuracy versus threshold for each classifier shown separately in Fig. B2). Net transfer entropy is found to be most accurate for classifying leader-follower relationships in simulated pairs of zebrafish. A threshold of 0.01 is found to be least accurate for both transfer entropy and time lag reaching 53% accuracy and a threshold value of 0.02 is found to be least accurate for event delay reaching 51% accuracy. The maximum accuracy for each of the methods is 87.5% for transfer entropy at a threshold value of 0.17, 53.5% for event delay at a threshold of 0.011, and 72.5% for time lag at a threshold of 0.08.

Transfer entropy has been used in fish behavioral studies to study predator-prey interactions in [30], and to elucidate the influence of a robotic stimulus on zebrafish behavior [28, 29, 31]. In the predator-prey study, transfer entropy is
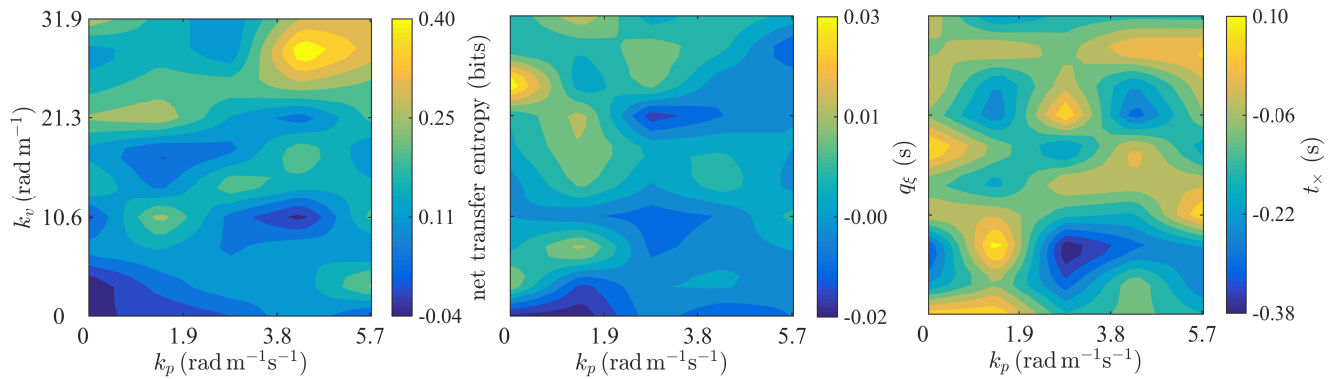
FIG. 7. Net transfer entropy, event delay (q_ξ), and time lag as a function of attraction and alignment gains k_p and k_v.

measured between a prey fish, *Rhodeus ocellatus*, and a predator fish, *Channa argus*, as they interact in an annular tank. In the robot studies, an externally actuated, preprogrammed replica was used to impose a unidirectional interaction toward live subjects, but was likely not perceived as a leader. Differently from these studies, where the nature of the interaction was not known, here we create leader-follower pairs by assigning empirically justified interaction parameters. This formulation affords the systematic analysis of the association between information flow, as measured by transfer entropy, and coupling gains, which is a first, necessary step toward the analysis of leader-follower relationships in fish schools.

VI. VARIATIONS IN COUPLING GAINS

To verify if a classifier is a reliable measure of leadership at varying coupling strengths, we systematically vary the gains in the intervals $k_v = [0, 31.9]\,\mathrm{rad\,m^{-1}}$ and $k_p = [0, 5.72]\,\mathrm{rad\,m^{-1}s^{-1}}$. These intervals represent the range of values obtained after fitting the model to experimental data. All other model parameters, including fish speed, are set equal to the average values obtained after fitting the model to experimental data (Table I in Appendix A).

To measure the strength of association, a correlation coefficient is computed between attraction and alignment gains, and each classifier. Specifically, 5 values of k_p and 10 values of k_v are selected to create 50 possible combinations of coupling gains to assign to the follower fish. Each of the three classifiers are then computed for all combinations. For each classifier, the correlation coefficient is calculated between all 50 values and the corresponding k_v or k_p values. Statistical significance is set at $p < 0.05$.

Figure 7 shows the variation in each of the classifiers as a function of attraction and alignment gains. Both net transfer entropy ($r = 0.251, p = 0.079$), and event delay ($r = -0.266, p = 0.062$) tend to correlate with the attraction gain, k_p, even if the correlation fails to reach statistical significance. On the other hand, time lag ($r = -0.106, p = 0.464$) is not correlated with the attraction gain (Fig. B3). With respect to alignment gain, k_v, net transfer entropy ($r = 0.561, p < 0.01$), and event delay ($r = 0.399, p < 0.01$) are both found to be correlated, while time lag is not ($r = 0.133, p = 0.359$).

Live zebrafish are expected to exhibit variability in their tendency to align and approach shoal members [63]. These tendencies are captured here by the variation in alignment and attraction coupling gains. Since we measure information transfer via change in orientation, it is likely that the classifier measures are more correlated to alignment gain, which directly maps the orientation to the desired turn rate in the response function (10), than the attraction gain. At the same time, the strong correlation of net transfer entropy with alignment gain demonstrates the feasibility of comparing the strengths of the causal relationships between different fish pairs towards reconstructing weighted dynamic networks [64].

VII. LEADERSHIP IN LARGER GROUPS

In its classical form, transfer entropy has at least two limitations that may affect its use to apprehend leader-follower relationships. First, fish behavioral response may be associated with information transfer through cues characterized by widely different temporal scales [39], which are difficult to resolve using the approach presented here. For example, fish may exhibit fear response in the form of a C- or S-start that occurs on the order of milliseconds [50], or in the

form of cessation of movement called freezing [39], that evolves over a few seconds [68]. Information transfer can be measured at multiple time-scales by incorporating a wavelet-based extension of transfer entropy [69], where wavelet coefficients of each process are used to define embedding vectors that are in turn used to compute transfer entropy. A second limitation is related to the data-intensive nature of this measure, which requires large datasets to compute reliable estimates of probability densities [70]. In this context, it may be beneficial to reduce the data dimensionality while preserving the essential dynamics. For instance, in the fish-robot interaction studies performed in [28, 29, 31] the dimension along the tank where the robot exhibits maximum variability in motion is utilized to compute transfer entropy, and in [30], a circular arena is divided into sixteen distinct compartments by partitioning along the angular and radial coordinates.

Extending this approach to groups of more than two individuals entails estimating net transfer entropy between pairs of fish, and then assessing leader roles by comparing across pairs. However, the identification of leader-follower pairs is likely to be subject to ambiguity from the possibility of indirect information transfer [71]. For instance, in a three-fish shoal, where fish 1 is a leader for 2 and 2 is a leader for 3, measuring information transfer through successive pairwise comparisons may suggest that a direct influence of fish 1 on 3. This is addressed in [71] by generalizing the notion of transfer entropy to include the extra information provided to a system by the other processes. The key challenge of this approach is the need of large dataset to accurately estimate probability density functions from empirical observations, which may be difficult to obtain in experimental observations. In a recent study, covert leaders were identified within simulated swarms on the basis of average conditional transfer entropy [72], which is transfer entropy conditioned on another process in order to remove its effect [73, 74], and was found to be less for leaders than followers [72].

VIII.   CONCLUSIONS

Fish schools have been considered for a long time as egalitarian societies [1, 4], in which coordination spontaneously emerges in response to external environmental stimuli. Recent studies have identified a number of behavioral and physiological variabilities among school members [6, 7, 11, 63, 65]. Such individual variations may be responsible for the appearance of leadership in the school [11]. However, understanding the causes and consequences of leadership is an open problem in the study of fish social behavior [52, 66]. Recent advances in vision-based, non-invasive fish tracking [67] have fueled a number of investigations to understand leader-follower relationships from individual trajectory data [15]. One way in which leadership can be inferred from trajectory observation is to identify the initiation of path-altering maneuvers within the group [11, 15]. However, such maneuvers typically last only a few milliseconds, with the time in between successive instances likely subject to specific traits of the individual. Further, the order in which they appear may not be preserved due to environmental disturbances, thus diluting the stability of individual roles across time segments.

Here, we demonstrate a new model-free information-theoretic approach to identify leader-follower relationships in zebrafish pairs from trajectory data. To reduce the effect of experimental confounds in the validation of our approach, we considered synthetic data of zebrafish pairs swimming in 2D. This dataset is generated by integrating the JPTW paradigm for zebrafish swimming with the social interaction model proposed in [33]. We compared our methodology with alternative techniques based on classical cross-correlation and nonlinear time-series analysis. Specifically, we classified trajectory datasets of leader-follower and leaderless pairs using: i) the model-free approach of measuring net transfer entropy, ii) extreme-event synchronization that assumes an underlying model for the occurrence of extreme events (sudden changes in orientation) in the trajectory data, and iii) time lags from cross-correlation. Our results show that net transfer entropy is the most accurate classifier to distinguish between leader-follower and leaderless pairs. Further, net transfer entropy correlates with the coupling strength of alignment for a wide parameter range, offering a reliable measure of leadership.

While our approach is demonstrated for the zebrafish animal model, the analysis can be extended to other social fish species and, in general, to other social organisms interacting through non-verbal cues. For example, the approach could be extended to pedestrian traffic, flocking birds, and herding ungulates. Our focus on zebrafish is motivated by the importance of this species in preclinical research, where it is rapidly becoming a species of choice for the analysis of functional and dysfunctional processes in humans [34, 36, 75]. As a result, a detailed understanding of the social behavior of this species bears a scientific value which may extend beyond this freshwater species, to unravel the neurobiological underpinnings of leader-follower interactions. We hypothesize that the possibility of interfering with zebrafish behavior using psychoactive compounds and genetic manipulations [35, 37], technological breakthroughs in high-throughput behavioral observations of zebrafish behavior [39, 76, 77], and advancements in the robust classification of social interactions will be critical for an improved understanding of leadership. Future work will seek to extend our approach to larger groups swimming in three dimensions, exploring the translational potential of the zebrafish model organism.

Appendix A: Further details on the model of zebrafish interactions
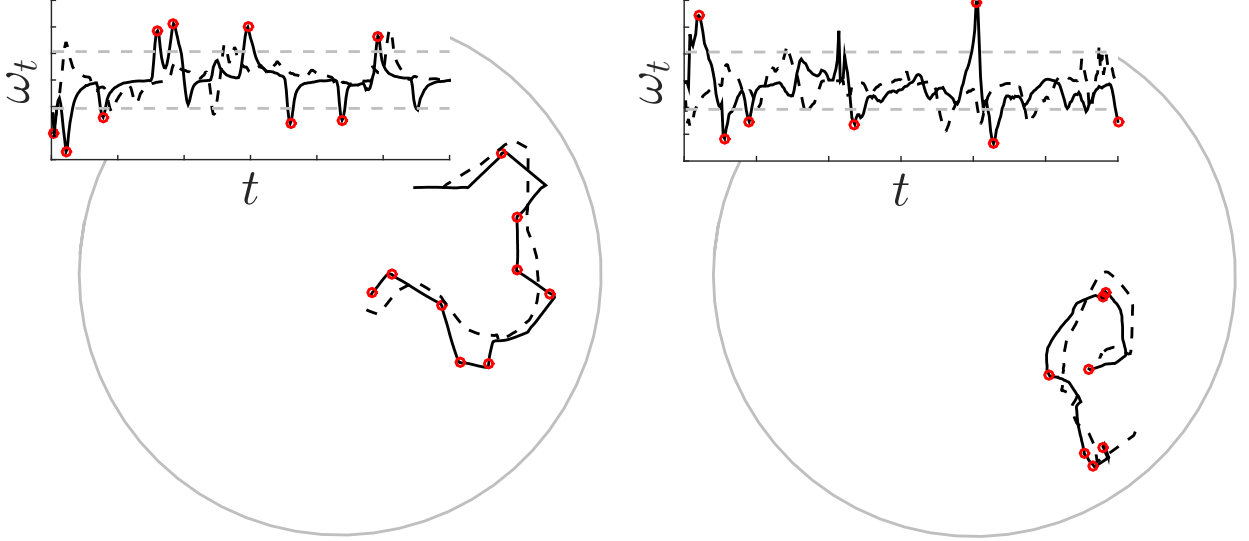
1. Experiments

FIG. A1. Sample fish trajectories, 10 seconds long, within the 90 cm diameter circular experimental area, with corresponding turn rates in the inset. Locations where turn rate is more than three standard deviations of the average turn rate are marked with red circles. Dataset obtained from [49].

The experimental dataset, collected as part of a previous study [49], comprises trajectories of pairs of zebrafish, filmed in a 120 cm × 120 cm tank using an overhead camera. Figure A1 shows sample trajectories with fast turns highlighted. A ring of diameter 90 cm was used to isolate a circular region within the tank where the fish were released. The fish were filmed at 30 frames per second as they swam in clear shallow water for twenty minutes, with the last ten minutes used for analysis. Individual fish were tracked using a multi-target tracking system [15], and the trajectories were verified and fixed manually if needed.

2. Model calibration

Combined, equations (8), (9), and (10) have seven parameters per fish (reversion rate, noise intensity, jump frequency, jump intensity, attraction gain, alignment gain, and speed), which should be determined using experimental data. Similar to [32, 41] we use nonlinear optimization to fit experimental data for each fish to the model. Specifically, with experimental trajectory data consisting of position $\mathbf{r}_k^{(i)}$, and orientation $\phi_k^{(i)}$ (represented by instantaneous direction of motion) sampled at time-steps $t_k, k = 1, 2, \ldots$, that are Δt apart, we compute the separation distance d_k, relative orientation $\phi_k^{(i,j)}$, and angular position $\theta_k^{(i,j)}$ as described in Section IV. Individual fish speed $v^{(i)}$ is set to the average speed during the experiment. These values are then used to estimate the turn rate $\omega_k^{(i)}$ in (8) and response function ${}^*\omega_{k-1}^{(i)}$ in (10). To find the parameters $\Theta^{(i)} = \left(\eta^{(i)}, \sigma^{(i)}, \gamma^{(i)}, \lambda^{(i)}, k_v^{(i)}, k_p^{(i)}\right) \in \mathbb{R}^6$, that best describe the change in turn rate in a maximum likelihood sense, we then minimize the sum of negative logarithms of the likelihood

function $\mathcal{L}\left(\omega_k^{(i)}|\omega_{k-1}^{(i)},\Theta^{(i)}\right)$ over all time-steps using *fmincon* routine in MATLAB (R2014b; MathWorks, Natick, MA, USA).
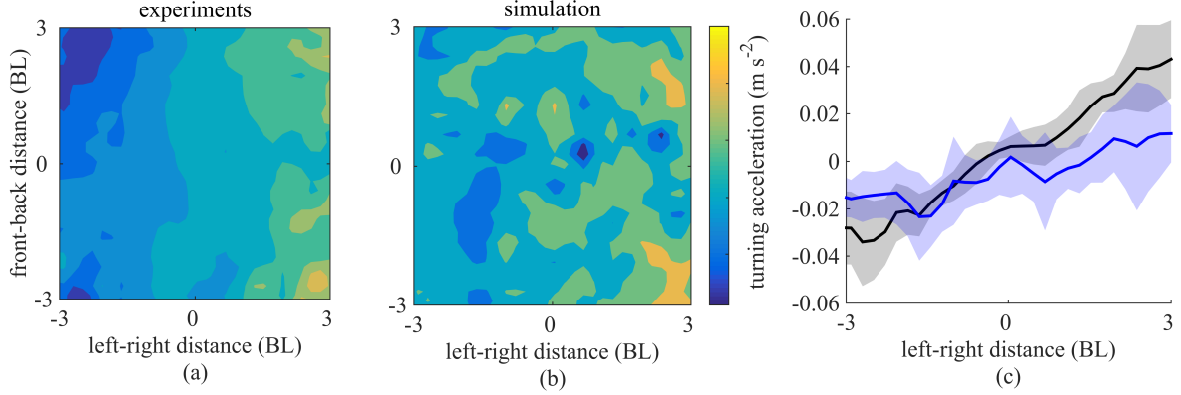

FIG. A2. Verification of the interaction model through the computation of the turning acceleration with respect to fish position in the body frame [18, 49] across all experimental (a) and simulated data (b). In the 2D histogram, (0,0) denotes the focal fish position, and the ordinate points in the direction of focal fish direction of motion. Each point (x,y) on the histogram represents an average of the turning acceleration of the focal fish across all times and all datasets, when the neighboring fish is in the (x,y) location. A simulation with the same model parameters obtained after the calibration is run per experimental dataset. Mean turning acceleration versus left-right distance (c) is shown for experimental (black) and simulated (blue) data, where each point on the graph represents a mean of all values across front-back distance for a given left-right distance from the focal fish. Color-bar has the same scale as the plot in (c), from -0.04 to 0.06 m s^{-2}.

In particular, denoting a Gaussian probability density function (pdf) with mean μ and variance var, evaluated at ω, as $\mathcal{N}(\omega;\mu,\text{var})$, the likelihood function is [32, 33][2]

$$\mathcal{L}\left(\omega_k^{(i)}|\omega_{k-1}^{(i)},\Theta^{(i)}\right) = \left(1-\lambda^{(i)}\Delta t\right)\mathcal{N}\left(\omega_k^{(i)};\mu^{(i)}\left(\omega_{k-1}^{(i)},\Delta t\right),\text{var}^{(i)}(\Delta t)\right) + \\ \lambda^{(i)}\Delta t\mathcal{N}\left(\omega_k^{(i)};\mu^{(i)}\left(\omega_{k-1}^{(i)},\Delta t\right),\text{var}^{(i)}(\Delta t)+\left(\gamma^{(i)}\right)^2\right),$$
(A1)

where

$$\mu^{(i)}\left(\omega_{k-1}^{(i)},\Delta t\right) = \omega_{k-1}^{(i)}e^{-\eta^{(i)}\Delta t} + {}^*\omega_{k-1}^{(i)}\left(1-e^{-\eta^{(i)}\Delta t}\right),$$
(A2)

and

$$\text{var}^{(i)}(\Delta t) = \frac{\left(\sigma^{(i)}\right)^2}{2\eta^{(i)}}\left(1-e^{-2\eta^{(i)}\Delta t}\right).$$
(A3)

Parameter values are constrained so that $\eta^{(i)}\in[1,2]\,\text{s}^{-1}$, $\sigma^{(i)}\in[1,5]\,\text{rad}\,\text{s}^{-3/2}$, and $\gamma^{(i)}\in[1,5]\,\text{rad}\,\text{s}^{-1}$ based on previously reported data [32]. The jump frequency is constrained as $\lambda^{(i)}\in[0.9,1.1]\lambda_0^{(i)}$ on the basis of the value $\lambda_0^{(i)}\left(\text{s}^{-1}\right)$ measured from trajectory data. The quantity $\lambda_0^{(i)}$ corresponds to the frequency of jumps in the turn rate of the i-th fish, which is estimated as the ratio between the number of time-steps when the absolute value of the turn rate is more than three standard deviations above the average and the total time duration of those time-steps. Note that $\lambda^{(i)}\Delta t$ measures the probability of a jump in the turn rate per time-step. The values of $k_p^{(i)}$ and $k_v^{(i)}$ are constrained in the broad range $[0,100]\,\text{rad}\,\text{m}^{-1}\text{s}^{-1}$ and $[0,100]\,\text{rad}\,\text{m}^{-1}$ respectively.

A total of 17 datasets, each comprising 10 minutes of trajectory data for two fish is used to obtain 34 sets of parameter values. To avoid extreme values in turn rate due to false measurements, points in fish trajectory where the absolute turn rate is more than 15 rad s^{-1} were removed [51]. This threshold is selected on the basis of maximum

---

[2] Note the unfortunate typo in [32, 41], where the variance is erroneously multiplied by Δt in the likelihood function and discrete-time approximation.

TABLE I. Parameter values obtained after calibrating the stochastic model for individual fish with interaction to data from 17 experiments, each with two fish. Average and standard deviation are computed over 34 parameter values. Note that the average speed refers to the entire dataset, beyond the 54 minutes used for calibration.

Parameter	Description	Value
η	Reversion rate	1.69 ± 0.32 s^{-1}
σ	Noise intensity	1.12 ± 0.18 rad s$^{-3/2}$
λ	Jump frequency	0.50 ± 0.09 s^{-1}
γ	Jump intensity	1.60 ± 0.40 rad s^{-1}
k_p	Attraction gain	1.29 ± 1.51 rad m^{-1}s^{-1}
k_v	Alignment gain	12.56 ± 7.41 rad m^{-1}
v	Speed	0.09 ± 0.02 m s^{-1}

observed turn rate measured indirectly from zebrafish swimming videos recorded at 5 frames per second [49, 51]. Such points correspond to less than 2 % of the total data. Further, to avoid wall effects and large changes from average speed that are not modeled by equations (8), (9), and (10), portions of trajectory where either fish is within 2 body lengths of the boundary wall, or individual speed is more than one standard deviation away from the average speed, are ignored. This corresponded to 67 % of the total dataset, leaving approximately 54 minutes of swimming time for calibration. Figure A1 shows pair of trajectories from two sample datasets with corresponding turn rates. Table I presents the average parameter values obtained after performing the model calibration. The difference in noise intensity and jump frequency values from previous studies on single zebrafish [32, 41] suggests that the presence of conspecifics affects the burst-and-coast swimming style of zebrafish.[3]

TABLE II. Parameter values after calibrating the stochastic jump model with interaction to each experimental dataset. For each parameter, the two columns correspond to the two different fish.

η (s^{-1})		σ (rad s$^{-3/2}$)		λ (s^{-1})		γ (rad s^{-1})		k_p (rad m^{-1}s^{-1})		k_v (rad m^{-1})		v (m s^{-1})	
1.08	2.00	1.01	1.00	0.49	0.55	1.40	1.70	0.00	0.22	9.00	9.31	0.08	0.06
2.00	2.00	1.00	1.00	0.57	0.59	1.14	1.34	1.35	0.00	8.84	5.72	0.06	0.06
1.56	1.55	1.00	1.00	0.45	0.58	1.20	1.37	1.32	0.48	9.76	9.76	0.13	0.13
1.65	1.60	1.04	1.04	0.47	0.39	1.66	1.65	0.00	5.14	15.11	7.97	0.08	0.08
1.42	1.43	1.25	1.27	0.45	0.41	1.86	1.83	0.00	0.00	16.72	15.63	0.08	0.09
1.51	2.00	1.18	1.00	0.39	0.54	1.55	1.42	5.73	1.77	13.70	11.39	0.10	0.11
1.77	2.00	1.12	1.00	0.51	0.68	1.38	1.28	0.58	2.80	16.02	5.55	0.06	0.06
2.00	2.00	1.00	1.00	0.55	0.57	1.30	1.30	2.52	1.35	9.04	8.65	0.08	0.08
1.71	1.08	1.46	1.65	0.60	0.40	2.15	2.64	0.00	3.25	17.88	31.19	0.06	0.07
1.21	1.47	1.21	1.00	0.52	0.41	2.87	1.43	2.29	1.78	26.50	5.33	0.08	0.08
2.00	2.00	1.00	1.00	0.70	0.43	1.12	1.23	0.00	2.59	14.16	3.72	0.08	0.09
1.32	1.85	1.32	1.00	0.37	0.55	1.86	1.26	3.89	0.00	25.02	13.83	0.07	0.07
1.33	1.54	1.09	1.00	0.62	0.34	1.51	1.63	1.96	0.07	17.25	9.70	0.10	0.10
1.87	2.00	1.61	1.09	0.56	0.46	1.99	1.25	0.00	1.70	7.76	7.90	0.08	0.08
1.63	2.00	1.00	1.49	0.51	0.52	1.99	2.15	0.49	1.87	3.31	0.66	0.13	0.16
2.00	1.00	1.00	1.09	0.71	0.30	1.21	1.47	0.09	0.00	5.50	31.90	0.11	0.13
2.00	1.96	1.07	1.17	0.57	0.47	1.74	1.59	0.54	0.00	16.86	16.55	0.09	0.09

3. Model selection

Compared to a model that does not include jumps as well as interaction, equation (9) includes four additional parameters, two for modeling the jump frequency and intensity and two for the interaction gains. To verify model

---

[3] Note that in [32, 41] λ is defined with respect to the time-step, so that the values presented therein should be multiplied by a 24 to compare with data in Table I; see experimental setup in [15].

selection, we accordingly use the Akaike information criterion (AIC) [78], that penalizes the number of parameters, n_p, to measure the model capability in fitting the data. Specifically, we compute the AIC for three model representations of fish turning rate: first a simple Ornstein-Uhlenbeck process comprising two parameters, a reversion rate η and noise intensity σ for each fish; second an interaction model without jumps as used in [48] that consists of four parameters; and third the combined interaction model with jumps.

For each model and corresponding likelihood function, AIC $= -2\ln(\mathrm{argmax}_{\mathbf{x}}\mathcal{L}) + 2n_p$. In the case of finite sample sizes, the corrected AIC value, which accounts for the number of samples, n_s, is AICc $=$ AIC $+$ $(2n_s(n_s+1))/(n_p - n_s - 1)$. Table III shows the AIC values for each of the three models. A one-way ANOVA comparison between the average AIC between models shows that an interaction model with jumps has a significantly lower AICc than a model that does not incorporate either jump or interaction ($p < 0.001$, F$(2, 99) = 6.72$). Post-hoc comparison using Fisher's honest significant difference test shows that AIC value of interaction with jump is significantly lower than the other two models.

TABLE III. AIC value for different models

Model	# of parameters	AIC
No interaction, no jumps	2	96.7 ± 104.2
Interaction, no jumps	4	100.6 ± 104.3
Interaction with jumps	6	12.0 ± 64.9

4. Model performance

To verify model integrity in comparison to experimental data, we compute turning acceleration defined as the component of acceleration perpendicular to the direction of motion as a function of neighbor position [18, 49]. Specifically, in a pair of fish, acceleration of the focal fish is projected onto a moving body frame whose origin lies on the fish position, and one of the axis, called the speeding axis, lies in the direction of motion; the axis normal to the speeding axis, called the turning axis, completes the frame. Turning acceleration is the component of fish acceleration that is projected on the turning axis. For a left (respectively right) position of the neighbor fish, the interaction model (10) adds a positive (respectively negative) value to the desired turn rate; this is reflected in the experimental data as well as the simulated data (Fig. A2).
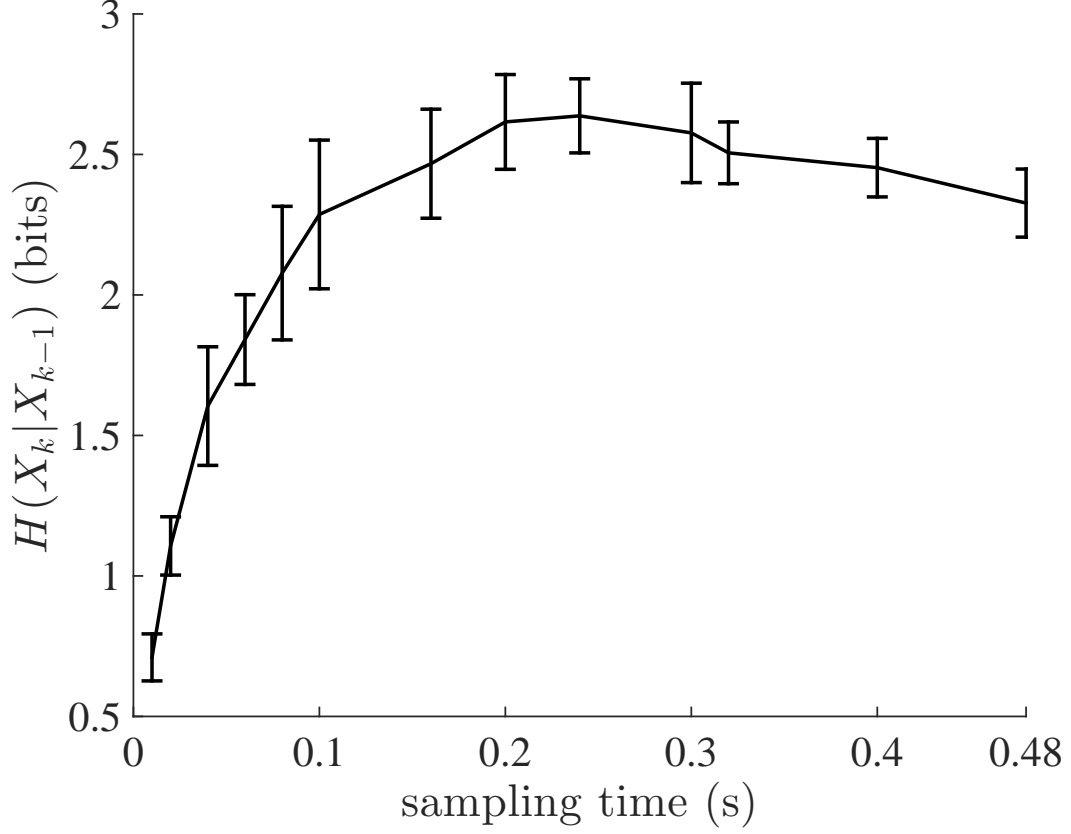
Appendix B: Additional figures

FIG. B1. Conditional entropy $H(X_k|X_{k-1})$, as a function of sampling time between steps. The conditional entropy increases significantly with increase in sampling time until 0.2 seconds. Error bars denote mean and standard deviation over 8 simulations.
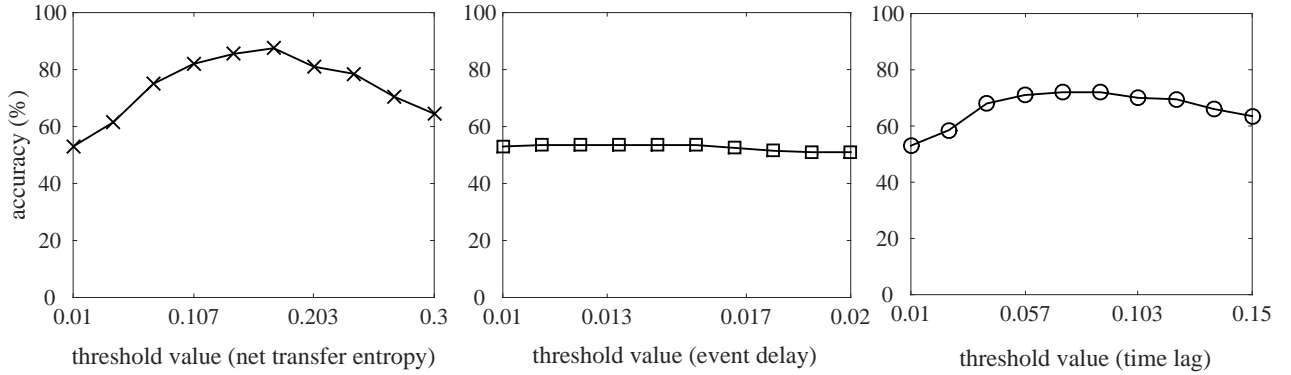

FIG. B2. Accuracy for each of the three classifiers—net transfer entropy, event delay, and time lag—as a function of threshold value.
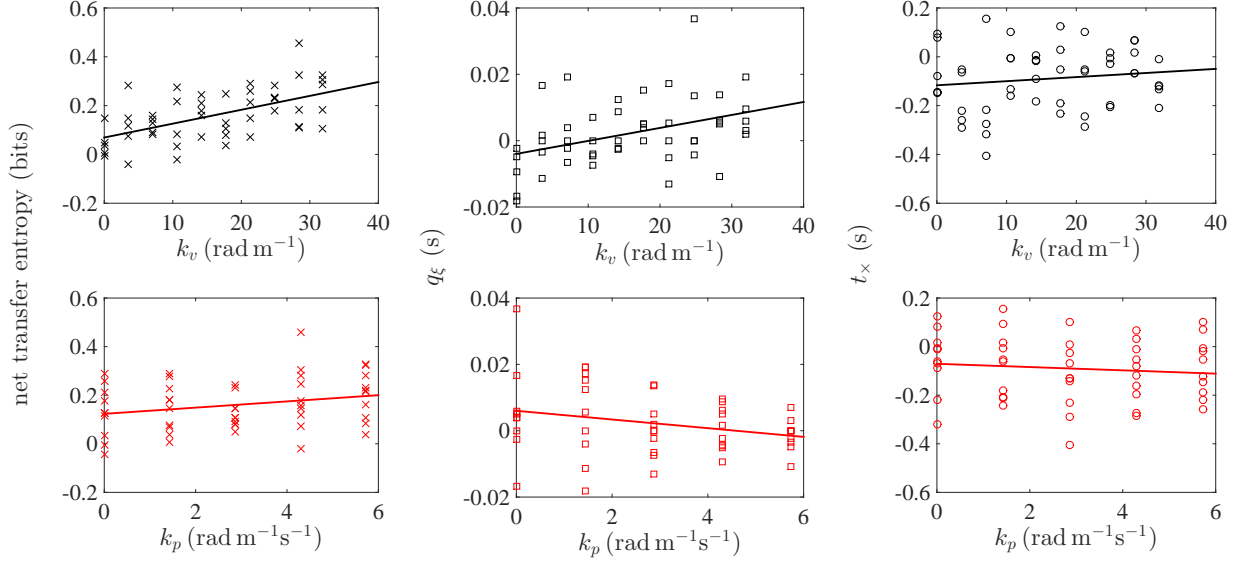
FIG. B3. Correlation of net transfer entropy, event delay, and time lag with alignment and attraction coupling gains. Correlation with alignment gain is performed over a range of attraction gains for each value. Similarly, correlation with attraction gain is computed over a range of alignment gains for each value. For alignment gain, all classifiers except time lag are correlated. For attraction gain, none of the classifiers are correlated.

[1] E. Shaw. Schooling fishes. *American Scientist*, 66(2):166–175, 1978.

[2] Peter F. Major. Predator-prey interactions in two schooling fishes, Caranx ignobilis and Stolephorus purpureus. *Animal Behaviour*, 26:760–777, August 1978.

[3] J. Herskin and J. F. Steffensen. Energy savings in sea bass swimming in a school: measurements of tail beat frequency and oxygen consumption at different swimming speeds. *Journal of Fish Biology*, 53(2):366–376, 1998.

[4] D. S. Wilson and E. Sober. Reviving the superorganism. *Journal of Theoretical Biology*, 136:337?356, 1989.

[5] A. Huth and C. Wissel. The simulation of the movement in fish schools. *Journal of Theoretical Biology*, 156(7):365–385, 1992.

[6] S. Marras, R. S. Batty, and P. Domenici. Information transfer and antipredator maneuvers in schooling herring. *Adaptive Behavior*, page 1059712311426799, 2011.

[7] S. Marras and P. Domenici. Schooling fish under attack are not all equal: some lead, others follow. *PLoS One*, 8(6):e65784, 2013.

[8] I. D. Couzin, J. Krause, N. R. Franks, and S. A. Levin. Effective leadership and decision-making in animal groups on the move. *Nature*, 433(7025):513–516, 2005.

[9] A. J. W. Ward, D. J. T. Sumpter, I. D. Couzin, P. J. B. Hart, and J. Krause. Quorum decision-making facilitates information transfer in fish shoals. *Proceedings of the National Academy of Sciences of the United States of America*, 105(19):6948–6953, 2008.

[10] C. M. Lindeyer and S. M. Reader. Social learning of escape routes in zebrafish and the stability of behavioural traditions. *Animal Behaviour*, 79(4):827–834, 2010.

[11] J. Krause, D. Hoare, S. Krause, C. K. Hemelrijk, and D. I. Rubenstein. Leadership in fish shoals. *Fish and Fisheries*, 1:82–89, 2000.

[12] C. Leblond and S. G. Reebs. Individual leadership and boldness in shoals of golden shiners (Notemigonus crysoleucas). *Behavior*, 143(10):1263–1280, 2006.

[13] J. L. Harcourt, T. Z. Ang, and G. Sweetman. Social feedback and the emergence of leaders and followers. *Current Biology*, 19(3):248–252, 2009.

[14] S. Nakayama, J. L. Harcourt, R. A. Johnstone, and A. Manica. Initiative, personality and leadership in pairs of foraging fish. *PLoS One*, 7(5):e36606, 2012.

[15] F. Ladu, S. Butail, S. Macrì, and M. Porfiri. Sociality modulates the effects of ethanol in zebrafish. *Alcoholism, Clinical and Experimental Research*, 38(7):2096–2104, 2014.

[16] N. W. F. Bode, D. W. Franks, and A. J. Wood. Leading from the front? social networks in navigating groups. *Behavioral Ecology and Sociobiology*, 66(6):835–843, 2012.

[17] N. Marwan and J. Kurths. Nonlinear analysis of bivariate data with cross recurrence plots. *Physics Letters A*, 302(5):299–307, 2002.

[18] Y. Katz, K. Tunstrøm, C. C. Ioannou, C. Huepe, and I. D. Couzin. Inferring the structure and dynamics of interactions in schooling fish. *Proceedings of the National Academy of Sciences of the United States of America*, 108(46):18720–18725, 2011.

[19] C. E. Shannon. A mathematical theory of communication. *The Bell System Technical Journal*, 27(1):379–423, 1948.

[20] K. Hlaváčková-Schindler, M. Paluš, M. Vejmelka, and J. Bhattacharya. Causality detection based on information-theoretic approaches in time series analysis. *Physics Reports*, 441(1):1–46, 2007.

[21] M. Zanin, E. Menasalvas, S. Boccaletti, and P. Sousa. Feature selection in the reconstruction of complex network representations of spectral data. *PLoS One*, 8(8), 2013.

[22] M. Timme and J. Casadiego. Revealing networks from dynamics: an introduction. *Journal of Physics A: Mathematical and Theoretical*, 47(34):343001, 2014.

[23] O. Stetter, D. Battaglia, J. Soriano, and T. Geisel. Model-free reconstruction of excitatory neuronal connectivity from calcium imaging signals. *PLoS Computational Biology*, 8(8):e1002653, 2012.

[24] R. Vicente, M. Wibral, M. Lindner, and G. Pipa. Transfer entropy–a model-free measure of effective connectivity for the neurosciences. *Journal of Computational Neuroscience*, 30(1):45–67, 2011.

[25] R. Kleeman. Information theory and dynamical system predictability. *Entropy*, 13(3):612–649, 2011.

[26] O. Kwon and J-S. Yang. Information flow between stock indices. *EPL (Europhysics Letters)*, 82(6):68003, 2008.

[27] G. Ver Steeg and A. Galstyan. Information transfer in social media. In *Proceedings of the International Conference on World Wide Web*, pages 509–518. ACM, 2012.

[28] S. Butail, F. Ladu, D. Spinello, and M. Porfiri. Information flow in animal-robot interactions. *Entropy*, 16(3):1315–1330, 2014.

[29] F. Ladu, V. Mwaffo, J. Li, S. Macrì, and M. Porfiri. Acute caffeine administration affects zebrafish response to a robotic stimulus. *Behavioural Brain Research*, 289:48–54, 2015.

[30] F. Hu, L.-J. Nie, and S.-J. Fu. Information dynamics in the interaction between a prey and a predator fish. *Entropy*, 17(10):7230–7241, 2015.

[31] T. Bartolini, V. Mwaffo, A. Showler, S. Macrì, S. Butail, S. and M. Porfiri. Zebrafish response to 3D printed shoals of conspecifics: the effect of body size *Bioinspiration & Biomimetics (in press)*, 2016

[32] V. Mwaffo, R. P. Anderson, S. Butail, and M. Porfiri. A jump persistent turning walker to model zebrafish locomotion. *Journal of the Royal Society Interface*, 12(102):20140884, 2015.

[33] J. Gautrais, F. Ginelli, R. Fournier, S. Blanco, M. Soria, H. Chaté, and G. Theraulaz. Deciphering interactions in moving animal groups. *PLoS Computational Biology*, 8(9):e1002678, 2012.

[34] G. J. Lieschke and P. D. Currie. Animal models of human disease: zebrafish swim into view. *Nature Reviews. Genetics*, 8(5):353–67, 2007.

[35] R. Gerlai. Using zebrafish to unravel the genetics of complex brain disorders. In *Current Topics in Behavioral Neurosciences, Behavioral Neurogenetics*, volume 12, pages 3–24. Springer Berlin Heidelberg, January 2012.

[36] A. V. Kalueff and A. M. Stewart, editors. *Zebrafish Protocols for Neurobehavioral Research*. Neuromethods. Humana Press, New York, New York, USA, 2012.

[37] M. Pham, J. Raymond, J. Hester, E. Kyzar, S. Gaikwad, I. Bruce, C. Fryar, S. Chanin, J. Enriquez, S. Bagawandoss, I. Zapolsky, J. Green, A. M. Stewart, B. D. Robison, and A. V. Kalueff. Assessing social behavior phenotypes in adult zebrafish: shoaling, social preference, and mirror biting tests. In *Zebrafish Protocols for Neurobehavioral Research: Neuromethods*, pages 231–246. Humana Press, Totowa, NJ, 2012.

[38] J. J. Videler. *Fish swimming*. Springer, 1993.

[39] A. V. Kalueff, M. Gebhardt, A. M. Stewart, J. M. Cachat, M. Brimmer, J. S. Chawla, C. Craddock, E. J. Kyzar, A. Roth, S. Landsman, S. Gaikwad, K. Robinson, E. Baatrup, K. Tierney, A. Shamchuk, W. Norton, N. Miller, T. Nicolson, O. Braubach, C. P. Gilman, J. Pittman, D. B. Rosemberg, R. Gerlai, D. Echevarria, E. Lamb, S. C. F. Neuhauss, W. Weng, L. Bally-Cuif, and H. Schneider. Towards a comprehensive catalog of zebrafish behavior 1.0 and beyond. *Zebrafish*, 10(1):70–86, 2013.

[40] T. Bartolini, V. Mwaffo, S. Butail, and M. Porfiri. Effect of acute ethanol administration on zebrafish tail beat motion. *Alcohol*, 49:721–725, 2015.

[41] V. Mwaffo and M. Porfiri. Turning rate dynamics of zebrafish exposed to ethanol. *International Journal of Bifurcation and Chaos*, 25(07):1540006, 2015.

[42] V. Mwaffo, S. Butail, M. diBernardo, and M. Porfiri. Measuring zebrafish turning rate. *Zebrafish*, 12(3):250–254, 2015.

[43] N. Miller and R. Gerlai. Quantification of shoaling behaviour in zebrafish (*Danio rerio*). *Behavioural Brain Research*, 184(2):157–166, 2007.

[44] N. Miller and R. Gerlai. From schooling to shoaling: patterns of collective motion in zebrafish (*Danio rerio*). *PLoS One*, 7(11):e48865, 2012.

[45] R. Q. Quiroga, T. Kreuz, and P. Grassberger. Event synchronization: a simple and fast method to measure synchronicity and time delay patterns. *Physical Review E*, 66(4):041904, 2002.

[46] V. Mwaffo, R. P. Anderson, and M. Porfiri. Collective dynamics in the vicsek and vectorial network models beyond uniform additive noise. *Journal of Nonlinear Science*, 25(5):1053–1076, 2015.

[47] J. Gautrais, C. Jost, M. Soria, A. Campo, S. Motsch, R. Fournier, S. Blanco, and G. Theraulaz. Analyzing fish movement as a persistent turning walker. *Journal of Mathematical Biology*, 58(3):429–445, 2009.

[48] D. S. Calovi, U. Lopez, S. Ngo, C. Sire, H. Chaté, and G. Theraulaz. Swarming, schooling, milling: phase diagram of a data-driven fish school model. *New Journal of Physics*, 16(1):015026, 2014.

[49] A. Zienkiewicz, D. A. Barton, M. Porfiri, and M. di Bernardo. Leadership emergence in a data-driven model of zebrafish shoals with speed modulation. *European Physical Journal*, 2015.

[50] R. C Eaton, R. A. Bombardieri, and D. L. Meyer. The mauthner-initiated startle response in teleost fish. *Journal of Experimental Biology*, 66(1):65–81, 1977.

[51] A. Zienkiewicz, D. A.W. Barton, M. Porfiri, and M. di Bernardo. Data-driven stochastic modelling of zebrafish locomotion. *Journal of Mathematical Biology*, 71:1081–1105, 2014.

[52] J. W. Jolles, A. Fleetwood-Wilson, S. Nakayama, M. C. Stumpe, R. A. Johnstone, and A. Manica. The role of social attraction and its link with boldness in the collective movements of three-spined sticklebacks. *Animal Behaviour*, 99:147–153, 2015.

[53] D. J. Higham. An Algorithmic Introduction to Numerical Simulation of Stochastic Differential Equations. *SIAM Review*, 43(3):525–546, 2001.

[54] C. W. J. Granger. Testing for causality: A personal viewpoint. *Journal of Economic Dynamics and Control*, 2(1):329–352, 1980.

[55] T. M. Cover and J. A. Thomas. *Elements of Information Theory*. John Wiley & Sons, New York, NY, USA, 2006.

[56] M. Vejmelka and M. Paluš. Inferring the directionality of coupling with conditional mutual information. *Physical Review E*, 77(2):026214, 2008.

[57] J. Hlinka, D. Hartman, M. Vejmelka, J. Runge, N. Marwan, J. Kurths, and M. Paluš. Reliability of inference of directed climate networks using conditional mutual information. *Entropy*, 15(1):2023–2045, 2013.

[58] T. Schreiber. Measuring information transfer. *Physical Review Letters*, 85(2):461–464, 2000.

[59] B. W. Silverman. *Density estimation for statistics and data analysis*. CRC press, Boca Raton, Florida, USA, 1986.

[60] N. Malik, B. Bookhagen, N. Marwan, and J. Kurths. Analysis of spatial and temporal extreme monsoonal rainfall over south asia using complex networks. *Climate Dynamics*, 39(3-4):971–987, 2012.

[61] J. Runge, J. Heitzig, V. Petoukhov, and J. Kurths. Escaping the curse of dimensionality in estimating multivariate transfer entropy. *Physical Review Letters*, 108(25):258701, 2012.

[62] P. Sonego, A. Kocsor, and S. Pongor. ROC analysis: applications to the classification of biological sequences and 3d structures. *Briefings in Bioinformatics*, 9(3):198–209, 2008.

[63] D. Wright, L. B. Rimmer, V. L. Pritchard, R. K. Butlin, and J. Krause. Inter and intra-population variation in shoaling and boldness in the zebrafish (*Danio rerio*). *Journal of Fish Biology*, 63(s1):258–259, 2003.

[64] S. Boccaletti, V. Latora, and Y. Moreno Complex networks: Structure and dynamics *Physics reports*, 424:175–308, 2006

[65] S. Marras, S. S. Killen, G. Claireaux, P. Domenici, and D. J. McKenzie. Behavioural and kinematic components of the fast-start escape response in fish: individual variation and temporal repeatability. *The Journal of Experimental Biology*, 214(Pt 18):3102–10, 2011.

[66] A. L. J. Burns, J. E. Herbert-Read, L. J. Morrell, and A. J. W. Ward. Consistency of leadership in shoals of mosquitofish (gambusia holbrooki) in novel and in familiar environments. *PLoS One*, 7(5):e36567–e36567, 2012.

[67] A. I. Dell, J. A. Bender, K. Branson, I. D. Couzin, G. G. de Polavieja, Lucas P.J.J. Noldus, A. Pérez-Escudero, P. Perona, A. D. Straw, M. Wikelski, and U. Brose. Automated image-based tracking and its application in ecology. *Trends in Ecology & Evolution*, 29(7):417–428, 2014.

[68] V. Kopman, J. Laut, G. Polverino, and M. Porfiri. Closed-loop control of zebrafish response using a bioinspired robotic-fish in a preference test. *Journal of the Royal Society Interface*, 10(78):20120540, 2013.

[69] M. Lungarella, M.Lungarella and Y. Kuniyoshi. Information transfer at multiple scales. *Physical Review E*, 76(5):056117, 2007.

[70] G. Gómez-Herrero, W. Wu, K. Rutanen, M. C. Soriano, G. Pipa, and R. Vicente. Assessing coupling dynamics from an ensemble of time series. *Entropy*, 17(4):1958–1970, 2015.

[71] J. Sun and E. M. Bollt. Causation entropy identifies indirect influences, dominance of neighbors and anticipatory couplings. *Physica D: Nonlinear Phenomena*, 267(1):49–57, 2014.

[72] Y. Sun, L. F. Rossi, C.-C. Shen, J. Miller, X. R. Wang, J. T. Lizier, M. Prokopenko, and U. Senanayake. Information transfer in swarms with leaders. *arXiv*, 2014.

[73] X. R. Wang, J. M. Miller, J. T. Lizier, M. Prokopenko, and L. F. Rossi. Quantifying and tracing information cascades in swarms. *PLoS One*, 7(7):e40084, 2012.

[74] J. T. Lizier, M. Prokopenko, and A. Y. Zomaya. Local information transfer as a spatiotemporal filter for complex systems. *Physical Review E*, 77(2):026110, 2008.

[75] A. M. Stewart, M. Nguyen, K. Wong, M. K. Poudel, and A. V. Kalueff. Developing zebrafish models of autism spectrum disorder (ASD). *Progress in Neuro-Psychopharmacology and Biological Psychiatry*, 50(0):27–36, 2014.

[76] R. Du, Z. Li, K. Youcef-Toumi, and P. V. y Alvarado. *Robot Fish: Bio-inspired Fishlike Underwater Robots*. Springer-Verlag Berlin Heidelberg, New York, 2015.

[77] A. M. Stewart, R. Gerlai, and A. V. Kalueff. Developing highER-throughput zebrafish screens for in-vivo CNS drug discovery. *Frontiers in Behavioral Neuroscience*, 9, 2015.

[78] E. Parzen, T. Kunio, and K. Genshiro editors Information theory and an extension of the maximum likelihood principle *Selected Papers of Hirotugu Akaike*. Springer Science & Business Media